

Inertial wave dynamics in a rotating and precessing cylinder

By J. JONATHAN KOBINE†

Department of Applied Mathematics and Theoretical Physics, University of Cambridge,
Silver Street, Cambridge, CB3 9EW, UK

(Received 4 May 1995 and in revised form 25 July 1995)

Results are presented from an experimental study of fluid in a rotating cylinder which was subjected to precessional forcing. The primary objective was to determine the validity of the linear and inviscid approximations which are commonly adopted in numerical models of the problem. A miniature laser Doppler velocimeter was used to make quantitative measurements of the flow dynamics under a variety of forcing conditions. These ranged from impulsive forcing to continuous forcing at the fundamental resonance of the system. Inertial waves were excited in the fluid in each case, with the extent of nonlinear behaviour increasing from one forcing regime to the next. Good agreement was found with the predictions of linear theory in the weaker forcing regimes. For stronger forcing, it was possible to determine the approximate duration of linear behaviour before the onset of nonlinear dynamics. Viscous effects were found to be relatively weak when the frequency of precessional forcing was away from resonance. However, there was evidence of strong boundary-layer phenomena when conditions of resonance were approached.

1. Introduction

A rotating body of fluid is capable of supporting a unique type of wave motion through the action of the Coriolis force. Such waves, known as *inertial waves*, may be found in problems as diverse as flow in the Earth's liquid core (Vanyo *et al.* 1995) and the dynamics of spin-stabilized projectiles (Herbert 1986). The particular application which motivated the present study is the stability of rotating spacecraft which carry liquid payloads. In such systems, excitation of inertial waves provides a non-dissipative mechanism by which angular momentum may be transferred between the solid spacecraft and its fluid contents. One possible consequence is that the spacecraft begins to nutate about its original orientation, with the angle of nutation growing exponentially with time (Stewartson & Roberts 1963; Rumyantsev 1964). At present, the approach to this problem is to fit baffles inside the tanks in such a way that the time constant for the nutational divergence is made manageably large. The optimal baffle configuration is generally obtained by means of free-fall experiments using scaled models of the liquid tanks (Pocha 1987). Such an approach is expensive and ultimately reveals little of the fundamental fluid mechanical processes which are involved.

A prerequisite for an efficient and reliable method for the design and control of rotating spacecraft is surely the ability to compute the motion of the on-board fluid

† Present address: Department of Atmospheric Physics, University of Oxford, Parks Road, Oxford, OX1 3PU, UK.

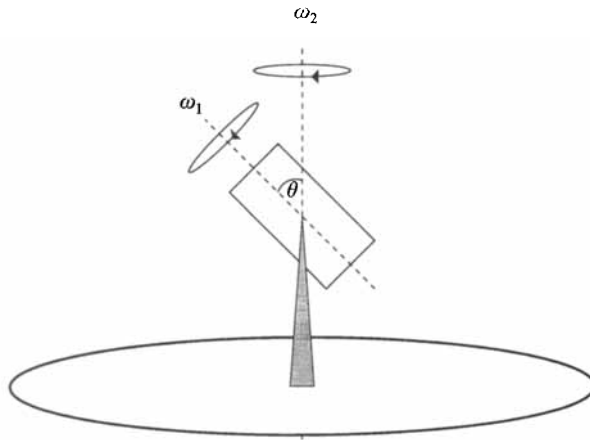


FIGURE 1. Schematic diagram of precessional forcing. Cylinder rotates with angular speed ω_1 relative to support. Support rotates at angular speed ω_2 relative to laboratory frame of reference.

and hence the effect on the vehicle as a whole. Mathematical difficulties associated with the existence of inertial oscillations prevent the application of classical techniques in all but a few special geometries. An alternative approach has been developed by Tan & McIntyre (1995), who have formulated the problem in terms of a time-dependent integral equation. However, in deriving their model, Tan & McIntyre adopted the standard linear and inviscid approximations in order to simplify the governing equations of motion. The relevance of such approximations may be questioned, since observations show that behaviour of a highly nonlinear character can develop when inertial oscillations are excited to a sufficient degree (McEwan 1970; Stergiopoulos & Aldridge 1982; Manasseh 1992). Hence the present experimental study was undertaken in order to establish the conditions under which forced inertial oscillations can be treated as linear behaviour, and the manner in which nonlinear effects develop.

Experiments were carried out using a right-circular cylinder which was completely filled with water and which rotated at a constant speed about its axis of symmetry. The right-circular geometry is one of the few cases where the linear inviscid model has an exact analytical solution (Greenspan 1968). The fluid response to an external force can be decomposed into a spectrum of normal modes, each with its own characteristic frequency which depends on the aspect ratio of the cylinder. Previous experimental investigations have confirmed the existence of such a spectrum, and have provided good agreement for values of the resonant frequencies (Fultz 1959) and resonant aspect ratios (McEwan 1970).

The choice of external forcing which was made by Tan & McIntyre (1995) and which is followed here was motivated by the observations of nutational behaviour in spacecraft and in free-fall simulations. Accordingly, forcing was applied by making the rotating cylinder precess at a constant speed about an axis passing through the centroid of the container (figure 1). In this way, the fluid inside the cylinder experiences a periodic force whose amplitude is controlled by the angle between the rotation and precession axes.

Previous investigations of inertial waves in a rotating cylinder have typically employed flow visualization, which is useful for revealing the spatial structure of flows but is generally unsuited for extracting dynamical information. In the few cases where dynamics have been studied, measurements have either been of relative pres-

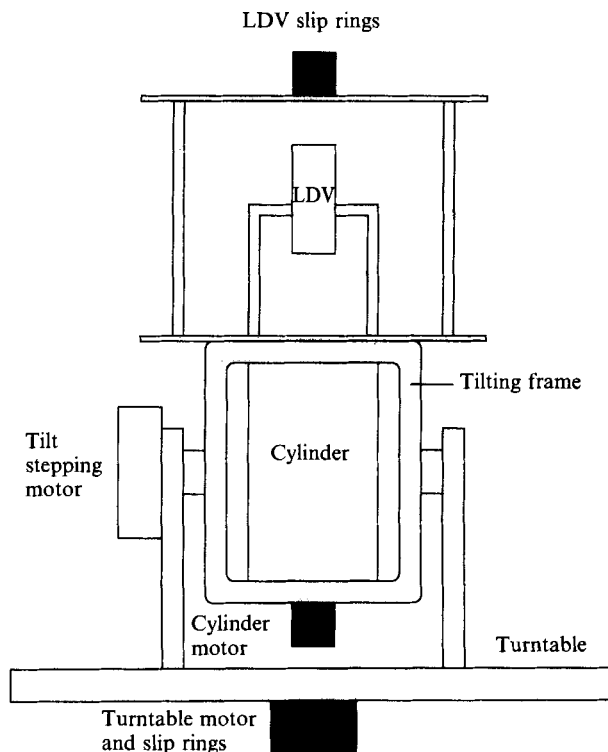


FIGURE 2. Sketch of the experimental apparatus.

sure fluctuations (Stergiopoulos & Aldridge 1982, 1987) or have involved intrusion into the flow (McEwan 1970). In the present study, measurements were made using a miniature laser Doppler velocimeter which allowed the flow speed at a point in the cylinder to be recorded directly without disturbing the flow in any way.

Several different forcing regimes were used in the experiments, such that the extent of nonlinear fluid behaviour was increased from one regime to the next. Initially, a quasi-impulsive force was applied by tilting the rotation axis of the cylinder suddenly through a small angle. Once the response of the fluid to such a force had been established, the effect of continuous non-resonant forcing was investigated by means of precession of the cylinder's axis of rotation. The strongest fluid response occurs when the precessional forcing is applied at the resonant frequency of the fundamental inertial mode. First, the fluid response immediately following the commencement of such forcing was considered. Then, the fully developed nonlinear behaviour associated with inertial-wave breakdown was investigated.

2. Experimental details

The purpose of this section is to give details of the experimental apparatus which was used in the study. The set-up is shown schematically in figure 2, and individual elements are described below.

2.1. Mechanical components

At the heart of the system was a right-circular cylinder which was filled completely with distilled water. The cylinder was made from Perspex, and had radius $a =$

45.00 ± 0.02 mm and height $H = 117.0 \pm 0.1$ mm. The aspect ratio for this cylinder was $h = H/2a = 1.300 \pm 0.002$. The cylinder was held in circular bearings inside a rigid frame, and could be rotated in either direction about its axis of symmetry by a 60 W d.c. motor via a 60:1 reduction gearbox. During the course of an individual experiment, the angular speed of the cylinder was stable to within 0.1% at a typical operating speed of $\omega_1 = 10 \text{ rad s}^{-1}$ relative to the rigid frame.

The supporting frame was mounted on a stand which allowed it be tilted about an axis running perpendicular to the axis of the cylinder and passing through the centroid of the cylinder. The angular position of the frame was set using a stepping motor connected to a 50:1 reduction gearbox. A single step of the motor corresponded to an angular increment $\Delta\theta = 0.018^\circ$. Tilts during all the experiments were controlled by a microcomputer, which turned the frame at a constant angular speed of $2.88^\circ \text{ s}^{-1}$ out to the required tilt angle θ .

The combined assembly of the cylinder and the supporting structure sat on a rotating turntable which was driven by a 180 W a.c. motor through a toothed belt drive. The angular speed ω_2 of the turntable in the laboratory frame of reference was typically in the range 1–3 rad s^{-1} and was found to be stable to within 0.2% during an individual experiment. The spin-up and spin-down of the turntable were under microcomputer control. A set of slip-rings allowed electrical power to be supplied to equipment on the turntable, as well as permitting signals to be received from the measuring devices.

The axis of rotation of the turntable bisected the axis of tilt of the right-circular cylinder. The majority of experiments began with the rotation axes of the cylinder and the turntable being coincident. This initial setting was performed manually with reference to a spirit level placed on the frame which contained the cylinder. It was found that the zero position set in this way was accurate to $\pm 0.1^\circ$. Conditions of either prograde or retrograde precession were achieved by setting the direction of rotation of the cylinder. When the cylinder and the turntable were rotating in the same direction ($\omega_1 > 0$, $\omega_2 > 0$) then there was prograde precession. If they were rotating in opposite directions ($\omega_1 < 0$, $\omega_2 > 0$) then there was retrograde precession. The definition of dimensionless forcing frequency Ω which is used throughout this paper is

$$\Omega = \frac{\omega_1}{\omega_1 + \omega_2}. \quad (1)$$

This definition is somewhat different from the one used by Manasseh (1992), but was chosen for the sake of consistency with the work of Tan & McIntyre (1995).

2.2. Laser Doppler velocimeter

A miniature laser Doppler velocimeter (LDV) was constructed specifically for these experiments. The LDV worked in the reference-beam mode of operation, and is shown schematically in figure 3.

The continuous output from an 8 mW infrared laser diode was directed into a cubic beam-splitter to produce two emergent beams. The straight-through beam had approximately 70% of the intensity of the original beam. The weaker perpendicular beam was brought parallel with the undeviated beam by a right-angled prism. Both the beam-splitter and the prism had optical coatings on their surfaces to reduce losses of intensity as light passed through the system.

The beams were focused by a plano-convex lens and passed through the upper face of the cylinder to intersect in the fluid. They were then reflected by a Perspex mirror which formed the lower face of the cylinder, and left through the upper face.

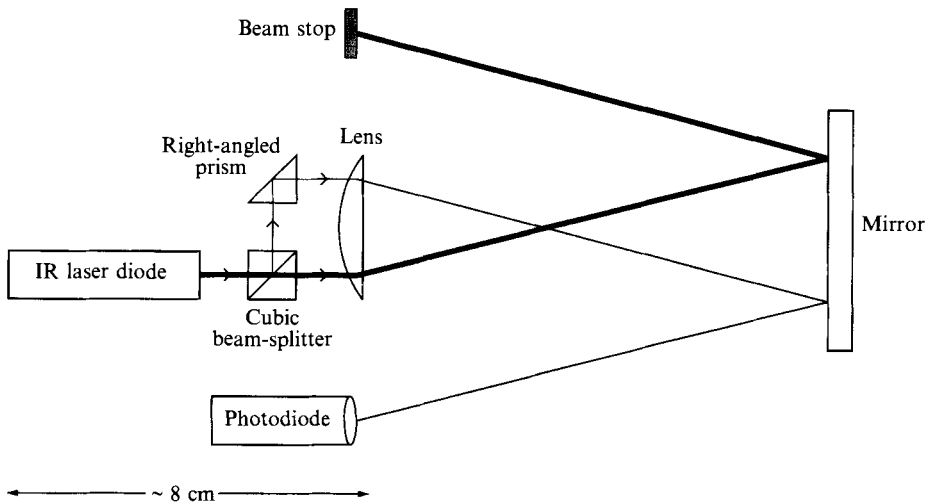


FIGURE 3. Schematic representation of the miniature laser Doppler velocimeter.

The stronger beam was blocked, while the weaker reference beam was picked up by a photodiode. The interference pattern which was established in the intersection volume had a fringe separation of $13.9 \mu\text{m}$. The fluid in the cylinder contained a small quantity (approximately 0.001% of the total volume) of latex spheres with diameter $11.9 \pm 1.9 \mu\text{m}$ and density 1.05 g cm^{-3} . These were included in order to enhance the Doppler signal. The particles were chosen to be of a similar size to the fringe spacing, and were essentially neutrally buoyant in water.

The entire LDV system was held in a mount which could be attached either to the cylinder or to the supporting frame. In this way, measurements could be made in the reference frame of either the cylinder or the turntable, while always ensuring that the LDV tilted with the rotation axis of the cylinder. A superstructure fixed to the frame (figure 2) held a set of slip-rings through which the signals from the rotating LDV were communicated to the turntable reference frame. The signal was then transmitted to the laboratory frame through the slip-rings in the turntable.

The laser Doppler velocimeter always measured the azimuthal component of the flow at the point of intersection of the beams. In order to keep the system as small and as light as possible, no mechanism was included for producing a difference in frequency between the two beams. The effect of this was that the Doppler signal could only be tracked by the electronics if there was sufficient flow (at least 10 mm s^{-1}) through the LDV measuring volume. The majority of the measurements which are reported in this paper were made with the cylinder rotating relative to the LDV. By measuring from this reference frame, the necessary through-flow was always present owing to the solid-body rotation of the fluid. However, measurements with the LDV rotating with the cylinder could be made under conditions where nonlinear boundary-layer effects produced a strong azimuthal circulation in the rotating frame. The reference frame from which measurements were made will be made clear in each case.

It is important to know the location of the LDV measuring volume when discussing certain of the experimental results. In all the experiments, the measuring point was fixed in the axial direction at a distance of 40 mm from the upper transparent face of the cylinder. The radial position was variable, and is quoted throughout in terms

of the dimensionless coordinate $r = r^*/a$. The azimuthal coordinate ϕ is measured relative to the axis about which the cylinder is tilted. Measurements were made at $\phi = 0$ in cases where the LDV was fixed to the frame containing the rotating cylinder.

2.3. Signal processing

The raw Doppler signal from the photodiode was first filtered to remove frequencies above 30 kHz. Doppler frequencies in this study were typically less than 10 kHz. The signal was then processed using a digital active bandpass filter (DABF) which tracked the strongest frequency component in the signal. This circuitry produced an output voltage that was directly proportional to the Doppler frequency and hence to the azimuthal flow speed at the measurement point. The output signal from the DABF was sampled by means of an 8-bit analogue-to-digital converter connected to a microcomputer.

It was found that the velocity signal produced when the cylinder rotated relative to the LDV contained a relatively high level of noise. This was due to intensity fluctuations caused by the double passage of the beams through the moving Perspex lid, together with the reflection off the moving mirror (although it should be noted that variations at the frequency of rotation were not observed). The noise level was reduced under these circumstances by the use of oversampling followed by averaging of the time series in a sequence of non-overlapping windows. Care was always taken to ensure that the effective sampling rate after windowing was still sufficiently high to give an unambiguous representation of the oscillations in the flow.

3. Free inertial oscillations

In this first set of experiments, the fluid in the rotating cylinder was supplied with a quasi-impulsive force in order to excite an inertial oscillation. In the absence of continued forcing, the excited mode was free to decay under the action of viscosity. Of primary interest were the fundamental frequency and the decay rate of the oscillation, since these quantities can be compared with the predictions of linear theory. Additional information was obtained which relates the amplitude of the response to the amplitude of the forcing.

3.1. Response to quasi-impulsive forcing

Experiments were performed at different values of cylinder speed ω_1 with the turntable speed $\omega_2 = 0$. In each case, the cylinder was left to rotate for a time well in excess of the spin-up time $a/(v\omega_1)^{1/2}$. Then, at a chosen moment, the axis of rotation was tilted at constant speed through an angle $\theta = 2.5^\circ$ in a time of 0.87 s. The fluid response in terms of the azimuthal flow speed was measured using the miniature LDV, which was fixed to the frame that held the rotating cylinder. The measuring position was located at $r = 0.14$. Sampling of the velocity time series was begun at the same instant that the tilt was initiated. Examples of the response following the above procedure are the dotted lines shown in figures 4(a) and 4(b) for $\omega_1 = 3.99$ and 10.84 rad s^{-1} respectively. The general behaviour in each case was oscillatory, with an amplitude envelope that decayed with time. The frequency and rate of decay were both greater for the larger value of ω_1 .

If it is assumed that a rotating body of fluid subjected to this form of forcing can be treated as a linear system which is weakly damped owing to the action of viscosity, then a possible model for the response in terms of the azimuthal speed $u(t)$ is

$$u(t) = u_{sbr} + A^* e^{-\beta^* t} \sin(\psi^* t + \epsilon) \quad (2)$$

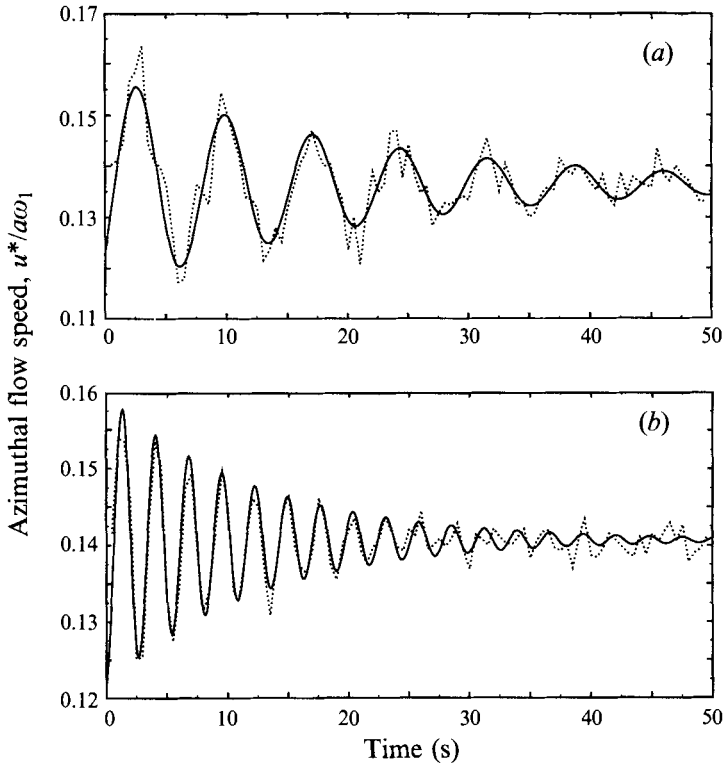


FIGURE 4. Time series showing fluid response to quasi-impulsive force in terms of azimuthal speed at a point in the flow: (a) cylinder speed $\omega_1 = 3.99 \text{ rad s}^{-1}$; (b) cylinder speed $\omega_1 = 10.84 \text{ rad s}^{-1}$. In each case, $\theta = 2.5^\circ$ and $\omega_2 = 0$. Dotted lines are experimental measurements; solid lines are least-squares fits of (2) to the experimental data.

for $t > 0$. The term u_{sbr} in (2) corresponds to the solid-body rotation speed which exists before the start of forcing at $t = 0$ and to which the system eventually returns once transient motions have decayed. The other term in (2) is a singly periodic oscillation with exponentially decaying amplitude as predicted by the linear theory of simple harmonic motion.

Least-squares fits were carried out of (2) applied to the experimental time series. The dimensional terms u_{sbr} , A^* , β^* , ψ^* and the dimensionless phase ϵ were all treated as free parameters of the fit. The fits for $\omega_1 = 3.99$ and 10.84 rad s^{-1} are the solid lines in figure 4(a, b). The behaviour prescribed by (2) is in qualitative agreement with that observed experimentally to within the limits set by the noise on the experimental time series. It would appear therefore that the fluid response to this quasi-impulsive force is, to a good approximation, singly periodic with exponentially decaying amplitude.

These time series are the quantitative equivalent of qualitative observations made by Manasseh (1992) under similar experimental conditions but using flow-visualization techniques. In that case, a sudden tilt of the cylinder's rotation axis was observed to produce a transient oscillation of the axial fluid core which decayed in a time comparable with the spin-up time. Free decay of inertial modes has also been studied experimentally in a different system by Stergiopoulos & Aldridge (1987). They investigated the behaviour in a rotating cylinder with a precessing lid where the fluid contents were spun-up from rest towards resonant conditions. The fluid

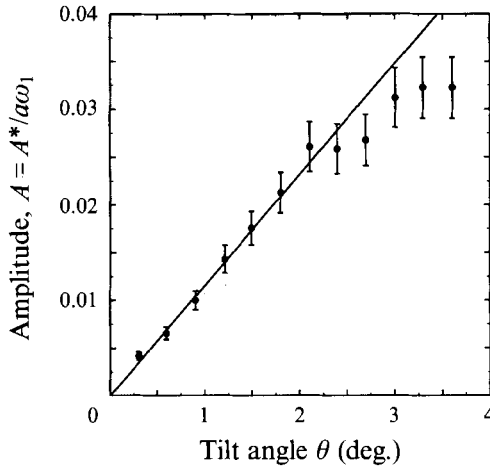


FIGURE 5. Variation of maximum amplitude of transient response with tilt angle θ . Solid line is least squares fit of $A = k\theta$ for $\theta < 2.5^\circ$.

response was measured in terms of the pressure difference between two points on the base of the cylinder. As the fluid spun up, an oscillation developed in the pressure signal, corresponding to an excited inertial mode. Once the oscillation amplitude had grown sufficiently, the forcing was switched off and the inertial mode was allowed to decay freely. The subsequent decrease in oscillation amplitude was found to be exponential. Measured values of frequency and decay rate agreed well with the linear theory appropriate to the problem.

3.2. Scaling properties of amplitude, frequency and decay rate

The above considerations show that the free decay of an inertial oscillation in a rotating cylinder can be regarded as a linear process to a good approximation. The response in terms of the azimuthal flow speed to a quasi-impulsive tilt of the rotation axis can be modelled by an exponentially decaying sinusoid as in (2). The next stage is to study the manner in which various terms in (2) depend on the experimental parameters.

The first relationship to be considered is that between the maximum amplitude of response and the tilt angle θ . A series of experiments was done with $\omega_1 = 10 \text{ rad s}^{-1}$ and $\omega_2 = 0$, in which the axis of rotation was tilted out to various angles θ at constant speed $d\theta/dt = 2.88^\circ \text{ s}^{-1}$. In each case, the resulting experimental time series was fitted with (2) and the value of A^* was noted. The results are shown in figure 5 in terms of the dimensionless amplitude $A = A^*/a\omega_1$. The data support a linear relationship between A and θ for values of $\theta < 2.5^\circ$. The results for larger tilt angles fall away from this linear trend, presumably because of the non-zero time required for the tilt to be completed. It is worth noting that all the other quantities which characterize the response proved insensitive to the value of θ .

A linear relationship between forcing amplitude and response amplitude was argued for by McEwan (1970) in the case of a rotating cylinder where the fluid is forced by a precessing lid. By assuming a balance between viscous dissipation and precessional forcing, McEwan showed that the 'steady state' oscillation amplitude q should satisfy a relationship of the form

$$\frac{q}{a\omega\alpha} \sim O(1). \quad (3a)$$

Here, ω is the cylinder rotation speed and α is the angle of inclination of the precessing lid. For the present results shown in figure 5, the dimensionless expression equivalent to (3a) is

$$\frac{A^*}{a\omega_1\theta} = 0.67, \quad (3b)$$

where θ is now in radians. This is in good agreement with the prediction made by McEwan using a steady-state assumption. Therefore, despite the fact that there is no steady state in the present problem, it appears reasonable to conclude that the maximum amplitude of the transient response is determined nevertheless by a balance between the quasi-impulsive force and viscosity.

The other scaling properties which are of interest concern the dependence of the frequency and decay rate of the oscillation on the rotation speed ω_1 . A second series of experiments was performed in which the cylinder speed was the only variable parameter. In each case, the rotation axis was tilted through a fixed angle $\theta = 2.5^\circ$. Least-squares fits of (2) were again employed, with the values of ψ^* and β^* recorded in each case.

The results plotted in figure 6(a,b) show the manner in which ψ^* and β^* depend on ω_1 . The data plotted in figure 6(a) support a direct linear relationship between ψ^* and ω_1 . The dimensionless response frequency is given by

$$\psi_t = \frac{\psi^*}{\omega_1} = 0.214 \pm 0.004, \quad (4)$$

where the uncertainty is derived from the least-squares fitting process. The subscript t indicates that this is a quantity measured from the turntable reference frame, which in this particular case is also the inertial reference frame since $\omega_2 = 0$. In the case of the decay rate, the results are plotted in figure 6(b) against $E^{1/2}\omega_1$, where the Ekman number E is defined as $E = \nu/a^2\omega_1$. This scaling supports a direct linear relationship, giving the dimensionless decay rate β as

$$\beta = \frac{\beta^*}{E^{1/2}\omega_1} = 1.125 \pm 0.025 \quad (5)$$

independent of the reference frame of measurement. Once again, the uncertainty is given by the fitting procedure.

3.3. Comparison with predictions of linear theory

The quantities given by (4) and (5) can be compared with results from linear theories appropriate to the problem under consideration. Firstly, for the dimensionless frequency ψ_t , it is necessary to take into account the Doppler shift due to the reference frame in which the measurements were made.

Consider the general case in which the cylinder is rotating with angular speed ω_1 and precessing with speed ω_2 . The nature of precessional forcing is such that all inertial modes which are excited have azimuthal wavenumber $m = 1$. Define ψ_c^* to be the dimensional angular frequency of an inertial mode measured from the reference frame which rotates with the cylinder. Using the fact that $m = 1$, it is easily established that

$$\psi_t^* = \omega_1 \pm \psi_c^*, \quad (6a)$$

where ψ_t^* is the dimensional frequency of the mode measured from the frame in which the cylinder rotates with speed ω_1 . The indeterminacy in the sign of ψ_c^* comes from the fact that there is no way of knowing *a priori* the azimuthal direction of

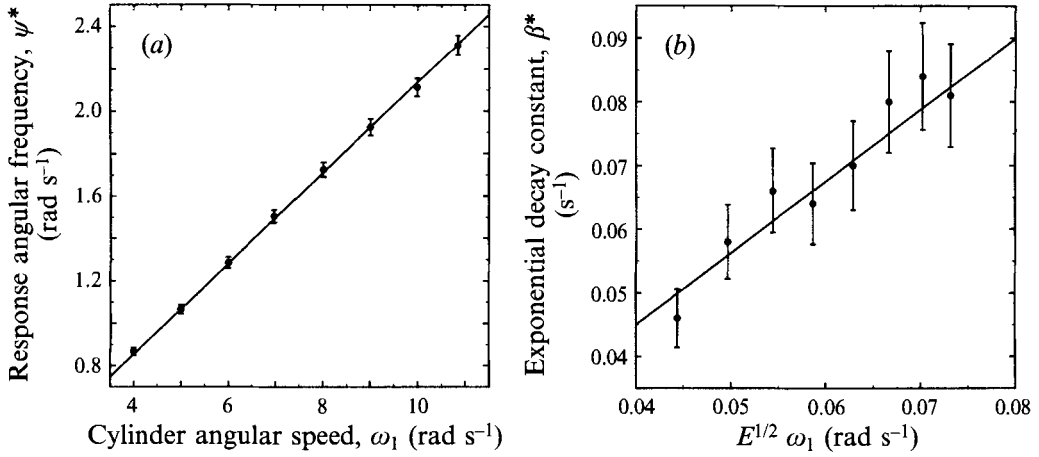


FIGURE 6. (a) Variation of angular frequency of transient response with cylinder rotation speed. Solid line is least-squares fit of $\psi^* = k\omega_1$. (b) Variation of exponential decay rate of transient response with cylinder rotation speed scaled by $E^{1/2}$. Solid line is least-square fit of $\beta^* = kE^{1/2}\omega_1$

propagation of the inertial mode. Non-dimensionalization of the terms in (6a) is achieved by dividing through by the quantity $\omega_1 + \omega_2$, giving

$$\psi_t = \Omega \pm \psi_c, \tag{6b}$$

with $\Omega = \omega_1/(\omega_1 + \omega_2)$ by definition in (1).

Returning to the present situation, we have $\omega_2 = 0$ and hence $\Omega = 1$. Using this value and rearranging (6b), we have

$$\psi_c = |1 - \psi_t|, \tag{7}$$

where now it is only the absolute value of ψ_c which is of practical interest. Substituting the value for ψ_t given by (4) into (7) gives an experimental value of

$$\psi_c = 0.786 \pm 0.004 \tag{8}$$

for the frequency of the oscillatory response to quasi-impulsive forcing that would be seen in the rotating reference frame.

The linear inviscid theory of inertial waves in a right-circular cylinder takes the form of a decomposition into a spectrum of normal modes (Kelvin 1880; Baines 1967; Manasseh 1992). The resonant frequencies of some of the lower-order modes have been calculated by Manasseh (1992) for the case of a cylinder with aspect ratio $h = 1.333$. In terms of the dimensionless frequency adopted here in (1), the frequency Ω_f of the fundamental inertial mode in a cylinder of aspect ratio h is given by

$$\Omega_f = 2 \left(1 + \left(\frac{2\lambda h}{\pi} \right)^2 \right)^{-1/2}. \tag{9a}$$

The term λ in (9a) is the first root of the equation

$$\lambda J_1'(\lambda) + \left(1 + \left(\frac{2\lambda h}{\pi} \right)^2 \right)^{1/2} J_1(\lambda) = 0, \tag{9b}$$

where $J_1(\lambda)$ is the Bessel function of the first kind of order 1.

Equation (9b) was solved numerically for the present case of a cylinder with aspect ratio $h = 1.300$, giving a value for the fundamental resonant frequency of

$$\Omega_f = 0.77639. \quad (10)$$

Johnson (1967) has shown that viscous effects result in a first-order correction of $O(E^{1/2})$ to the frequencies of inertial modes in a cylinder. In the context of the present problem, this constitutes a discrepancy of approximately 2% of the frequency of the fundamental inertial mode in the absence of viscosity. This is greater than the difference between the experimental value in (8) and the inviscid theoretical value in (10), and so it is concluded that the observed fluid response does in fact correspond to the fundamental inertial mode of the system.

A linear theory for the decay of inertial waves due to viscous dissipation has been formulated by Greenspan (1964) and Kudlick (1966). The essential elements of this theory are summarized by Greenspan (1968). The main prediction of the theory is that all contained inertial modes should decay in the spin-up time scale $t = (E^{1/2}\omega_1)^{-1}$. In other words, the dimensionless decay rate $\beta = \beta^*/(E^{1/2}\omega_1)$ should have values

$$\beta \sim O(1). \quad (11)$$

This prediction is supported by the experimental value of $\beta = 1.125 \pm 0.025$ given in (5).

4. Forced inertial oscillations away from resonance

The results presented in §3 show that the response of fluid in a rotating cylinder to a quasi-impulsive force takes the form of the excitation and subsequent viscous decay of the fundamental inertial mode in the system. The objective in this section is to establish the nature of the response when a quasi-impulsive force is combined with a continuous non-resonant precessional force.

Experiments were performed with the cylinder rotating at $\omega_1 = 10 \text{ rad s}^{-1}$ relative to the turntable and the turntable itself rotating at various values of ω_2 relative to the laboratory frame of reference. Initially, the two axes of rotation were coincident and the fluid in the cylinder was in solid-body rotation. Then, at time $t = 0$, the cylinder axis was tilted out to an angle $\theta = 2.5^\circ$ relative to the turntable axis and subsequently held fixed. The LDV was mounted so as to tilt with the cylinder, but was otherwise stationary in the frame of reference of the rotating turntable. Conditions of both prograde ($\Omega < 1$) and retrograde ($\Omega > 1$) precession were employed, and the fluid response was recorded at values of the dimensionless forcing frequency Ω ranging from 0.82 to 1.10. The radial measuring coordinate in each case was $r = 0.24$.

A typical time series which was recorded experimentally is shown in figure 7 for $\Omega = 0.86$. There are two distinct frequency components in the response. One is a decaying oscillatory component similar to the transient behaviour which was observed in §3. The other component is of higher frequency, and corresponds to the precessional forcing which the fluid experiences with frequency $\omega_1/2\pi$.

It is found that the slow oscillation is accurately described by (2). The result of a least-squares fit of (2) to the experimental time series is shown as the solid line in figure 7. As was the case in §3, the impulsive tilt excites a basic oscillation which then decays exponentially. The effect of the precessional forcing is a persistent secondary oscillation which appears as a linear superposition on the transient response.

The angular frequency ψ_i^* of the exponentially decaying oscillation was noted for each value of Ω at which experiments were performed. The dimensionless frequency

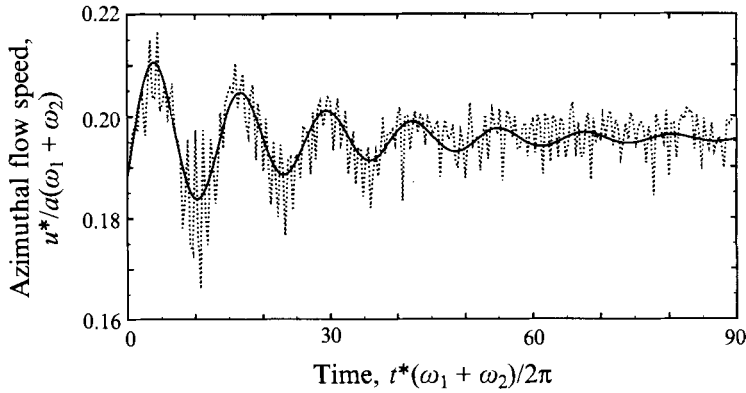


FIGURE 7. Time series showing fluid response to quasi-impulsive force combined with continuous non-resonant precessional force. Cylinder speed $\omega = 10.0 \text{ rad s}^{-1}$, turntable speed $\omega_2 = 1.63 \text{ rad s}^{-1}$, tilt angle $\theta = 2.5^\circ$. Dotted line is experimental measurement; solid line is least-squares fit of (2) to experimental data.

ψ_t is defined as $\psi_t = \psi_t^*/(\omega_1 + \omega_2)$. The results which were obtained are shown in figure 8. An expression for the expected variation of ψ_t with Ω has already been given by (6b) in §3.3. If it is assumed that the decaying oscillation which is observed in each case corresponds to the fundamental inertial mode, then the value for ψ_c in (6b) can be taken as the experimental value given by (8). The straight line drawn in figure 8 is a representation of the expression

$$\psi_t = \Omega - 0.786 \quad (12)$$

obtained from (6b) and (8). There is certainly very good agreement between (12) and the measured values of ψ_t over the majority of the range of Ω which was studied. Such agreement clearly resolves the indeterminacy of sign in (6b). The departure of the data points from the straight line for values of Ω approaching 0.8 is due to the existence of a mean azimuthal circulation which appears when the forcing frequency approaches the resonant frequency of the fundamental mode. This mean-flow phenomenon has been investigated in detail, and will be described in a future publication (Kobine 1995). The effect of the circulation is to introduce a Doppler shift in addition to the trivial one argued for in §3.3 and represented by (12).

5. Forced inertial oscillations at resonance

We turn now to consider the immediate response of fluid in a rotating right-circular cylinder when it is forced precessionally at frequencies close to the resonant frequency of the fundamental inertial mode. Initially, the qualitative features of the response will be described. This is followed by experimental data which provide evidence for linear behaviour in the fluid motion immediately after the onset of forcing.

5.1. Qualitative features of the response

The experiments of this section were similar in many respects to those described in §4. The cylinder speed was fixed at $\omega_1 = 10 \text{ rad s}^{-1}$ and values of the turntable speed were chosen to give the required values of Ω . The conditions at the start of every experiment were that the two axes of rotation were coincident and that the fluid was in solid-body rotation. The difference here is that measurements were made with the

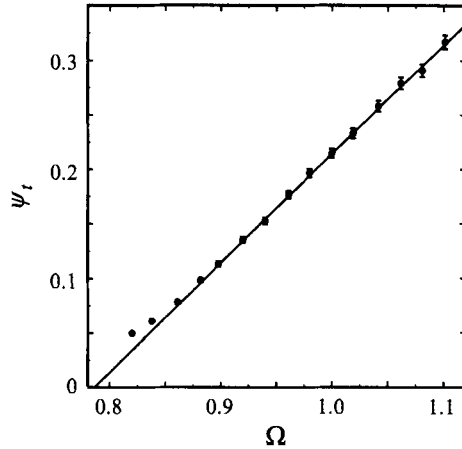


FIGURE 8. Variation of angular frequency of transient response with dimensionless forcing frequency Ω . Solid line is obtained from analytical expression given in (12).

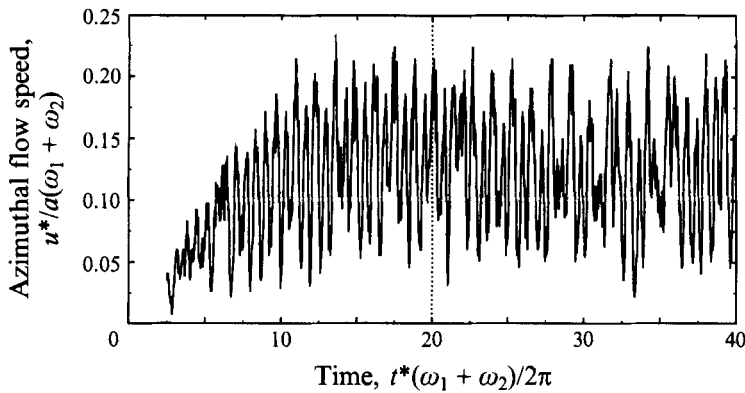


FIGURE 9. Experimental time series showing variation in azimuthal flow speed following onset of resonant precessional forcing. Cylinder speed $\omega_1 = 10.0 \text{ rad s}^{-1}$, turntable speed $\omega_2 = 2.79 \text{ rad s}^{-1}$, tilt angle $\theta = 2.0^\circ$. Measurement made from reference frame rotating with the cylinder. Dotted line indicates approximate time for inertial-wave breakdown as determined by Manasseh (1992) using flow-visualization techniques.

LDV attached directly to the cylinder so that the measurement point was fixed in the frame of reference rotating with speed $\omega_1 + \omega_2$. The measurement point was located at $r = 0.19$ in each case.

A typical time series showing the response in terms of the azimuthal flow speed is shown in figure 9 for frequency $\Omega = 0.782$ and tilt angle $\theta = 2.0^\circ$. Time $t = 0$ corresponds to the time at which the tilt was initiated. The response consists of an oscillation on top of a mean flow, both of which grow with time initially. The absence of data in the earliest stages is due to insufficient flow through the LDV measurement volume. However, a sufficient through-flow is soon established by the growth of the mean circulation. After $t \approx 20$, the growth of both the amplitude and the mean flow appear to have saturated. The subsequent behaviour is characterized by an irregular oscillation about an approximately constant non-zero mean.

Experiments similar to those described above have been performed by Manasseh (1992) using flow visualization to obtain information about the fluid motion. Forcing

close to the fundamental resonance produced an initial wave form which could be identified as the fundamental mode by its spatial structure. After a short time, the wave form developed some local instabilities. This was followed almost immediately by a violent collapse to small-scale structure throughout the fluid. It proves instructive to relate such observations and measurements to the present LDV measurements of the same phenomenon.

The dotted line in figure 9 marks the approximate time for breakdown of the inertial mode which is to be expected on the basis of the results Manasseh (1992). He measured the time from the onset of precessional forcing until the appearance of small-scale structure. Timings are available for values of Ω close to the fundamental resonance at tilt angles $\theta = 1.0^\circ$ and 3.0° . The time that is marked here for $\theta = 2.0^\circ$ is a linear interpolation. Referring to figure 9, it is apparent that the breakdown of the inertial mode occurs at approximately the same time as saturation of the growth of both the oscillation amplitude and the mean flow. What is not apparent is the violent nature of the breakdown as observed using flow visualization. Measurements made using the LDV, such as those shown in figure 9, show a continuous evolution from regular to irregular behaviour. Indeed, it will be seen in §6 that even in the fully developed nonlinear regime the dynamics of the flow are much simpler than at first suggested by flow visualization experiments.

A possible explanation for this discrepancy is related to the reference frames in which the observations and measurements were made. The flow-visualization studies carried out by Manasseh (1992) were made from the reference frame of the turntable. A stationary sheet of light was shone through the rotating cylinder to illuminate the visualization material in the flow. In the present case, the LDV rotated with the cylinder and thus measured the dynamics in the rotating reference frame. Any spatial structure in the azimuthal direction which is fixed in the cylinder frame of reference would not affect the LDV measurements, but would be visible as it passed through the light sheet of Manasseh's study. Some qualitative experiments were done using flow visualization and observing from the frame of the cylinder. The breakdown phenomenon observed in this way certainly appeared less violent, and there was evidence for stationary azimuthal structure. However, it would require considerably more investigation before a definite answer to the question could be given.

5.2. Growth of inertial oscillation amplitude with time

The oscillation amplitude is determined by locating successive maxima and minima in the time series, and then taking the difference to obtain a peak-to-peak amplitude. The results of such a procedure applied to the time series in figure 9 are plotted in figure 10. The data support a linear growth of amplitude with time up to $t \approx 10$ to within the limits of the experimental error. This can be seen from the straight line through the origin of figure 10. After $t \approx 10$, the growth of the oscillation saturates owing to nonlinear effects which develop for sufficiently large amplitude.

The linear growth rate of the amplitude of the inertial oscillation can be expected to depend on the external experimental parameters. In particular, the variation of growth rate has been studied here for fixed Ω and varying θ , and also for fixed θ and varying Ω . The results of these two experimental tests are presented below.

5.3. Variation of amplitude growth rate with θ

Experiments of the type described in §5.1 were carried out with $\Omega = 0.782$ for values of θ ranging from 0.5° to 3.0° . In each case the initial growth of oscillation amplitude from zero was found to be linear as illustrated in §5.2. The dimensional linear growth

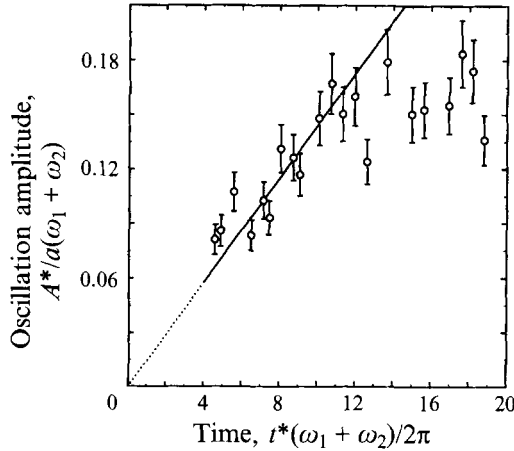


FIGURE 10. Variation of peak-to-peak oscillation amplitude following onset of resonant precessional forcing. Experimental parameters as for figure 9. Solid line is least-squares fit of $A = kt$ to data for $t < 10$.

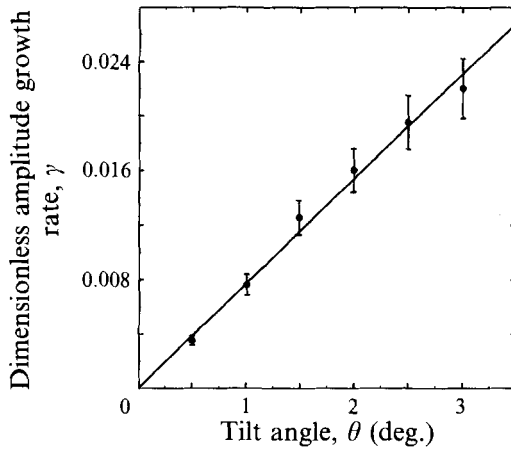


FIGURE 11. Variation of dimensionless amplitude growth rate γ of inertial oscillation with tilt angle θ for $\Omega = 0.782$. Solid line is least-squares fit of $\gamma = k\theta$ to the experimental data.

rate γ^* was obtained by applying a least-squares fit to the appropriate section of the data sets equivalent to that shown in figure 10 for $\theta = 2.0^\circ$. The dimensionless growth rate γ is defined here as

$$\gamma = \frac{2\pi\gamma^*}{a(\omega_1 + \omega_2)^2}. \quad (13)$$

The values of γ which were obtained experimentally are plotted against θ in figure 11. It can be seen that the oscillation amplitude grows faster for larger values of tilt angle. The data plotted in figure 11 support a relationship of the form $\gamma = 0.44\theta$ (with θ in radians) over the range of θ which was investigated.

The rate at which the oscillation amplitude grows initially can be related qualitatively to the time taken for the oscillation to break down to irregular behaviour. Manasseh (1992) measured the resonant breakdown time of the fundamental inertial mode at tilt angles θ from 0.3° to 5° . In those experiments, the breakdown time was found to decrease monotonically with increasing θ . This is in accord with the present

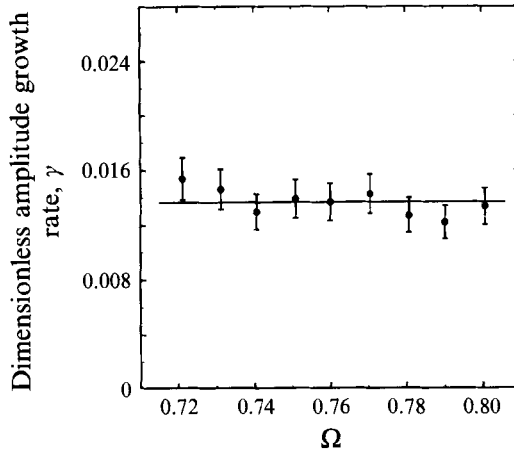


FIGURE 12. Variation of dimensionless amplitude growth rate γ of inertial oscillation with dimensionless forcing frequency Ω for $\theta = 2.0^\circ$. Solid line is least-squares fit of $\gamma = k$ to the experimental data.

data, which show the initial growth rate to be directly proportional to θ . As such, it can be expected that the nonlinear effects which lead to breakdown are encountered sooner for larger values of θ .

5.4. Variation of amplitude growth rate with Ω

Measurements were also made to look for any variation of the growth rate γ with forcing frequency Ω at fixed precession angle θ . The range of the value of Ω from 0.72 to 0.80 was chosen to include the fundamental resonance at $\Omega = 0.786$. In each case, the cylinder axis was tilted out to an angle $\theta = 2.0^\circ$ relative to that of the turntable. The fluid response was measured at $r = 0.19$ with the LDV rotating with the cylinder. Values of the linear amplitude growth rate were obtained in the manner described in §5.3.

The results of the above experimental procedure are plotted in figure 12. The data indicate that, at least to within experimental error, the amplitude growth rate γ is insensitive to the forcing frequency Ω over the range that was studied. This is in contrast to the behaviour observed when Ω is fixed but θ is varied, as shown in figure 11. The slight discrepancy in the value of γ at $\theta = 2.0^\circ$ between figures 11 and 12 is due to a small difference in the measuring position r between the two sets of experiments.

As was the case in §5.3, it is again possible to compare the variation of γ with that of the breakdown time as measured by Manasseh (1992). Values of the breakdown time are available for $\theta = 0.4^\circ, 1^\circ$ and 3° over a range of forcing frequency around the fundamental resonance equivalent to the one studied here. The results obtained by Manasseh for each of the three angles show relatively little variation in the breakdown time with forcing frequency. Once again, this is in agreement with the LDV measurements being reported here.

6. Features of the fully developed nonlinear regime

The final stage of the present study was an attempt to uncover features which might be relevant to understanding the fully developed nonlinear response of fluid subjected to precessional forcing following the breakdown of inertial modes. Previous

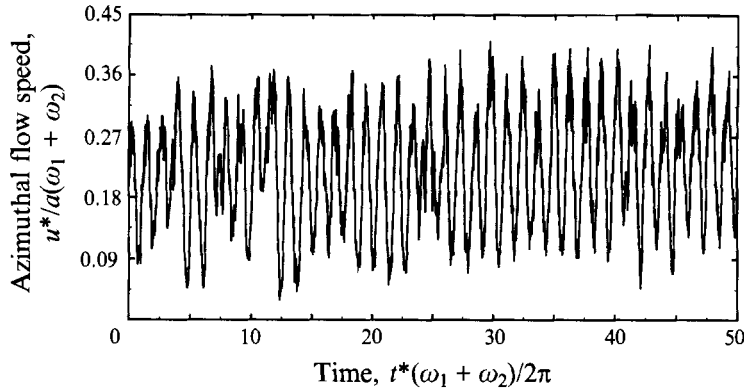


FIGURE 13. Time series recorded in regime of fully developed nonlinear behaviour following breakdown of inertial oscillations at $\Omega = 0.781$. Cylinder speed $\omega_1 = 10.67 \text{ rad s}^{-1}$, turntable speed $\omega_2 = 2.99 \text{ rad s}^{-1}$, tilt angle $\theta = 4.0^\circ$. Reference frame rotating with cylinder.

experimental investigations of this phenomenon (McEwan 1970; Manasseh 1992, 1993; Vanyo *et al.* 1995) and the related phenomenon of elliptical flow instabilities (Malkus 1989; Gledzer & Ponomarev 1992) have used flow-visualization techniques and have necessarily been directed towards describing the spatial characteristics of flows which have broken down into irregular behaviour. The aim in the present case was to investigate the dynamics of such flows in an attempt to identify any underlying mechanism which might possibly be responsible for the observed behaviour.

During these experiments, the miniature LDV system was used to measure the flow dynamics in the fully nonlinear regime. The cylinder rotation speed was set at $\omega_1 = 10.67 \text{ rad s}^{-1}$, while the turntable speed was chosen to be $\omega_2 = 2.99 \text{ rad s}^{-1}$. These two speeds give a value of $\Omega = 0.781$ for the dimensionless forcing frequency. This is very close to the resonance frequency associated with the fundamental inertial mode ($\Omega = 0.786$). Each experiment began with the two axes of rotation being coincident and the fluid moving in solid-body rotation. The cylinder was then tilted out and held at an angle θ relative to the axis of precession. The LDV system was attached so that it rotated with the fluid-filled cylinder. The measuring position was located at $r = 0.39$ in each case.

In order to determine when the flow is fully developed, it is useful to refer to work carried out previously by Manasseh (1992) on the breakdown of inertial waves in a rotating and precessing right-circular cylinder. The breakdown time was taken by Manasseh as the time from the onset of precessional forcing to the appearance of small-scale spatial structure in the flow, measured in units of $2\pi/\omega_1$. For a forcing amplitude of $\theta = 1.0^\circ$, the dimensionless breakdown time close to resonance was found to be approximately 22 units.

In the present case, the system was left precessing for dimensionless times of at least 120 units in order to ensure that all breakdown events and any associated transient behaviour had passed. Once such a time had elapsed, the time series of azimuthal velocity was recorded for approximately 500 dimensionless time units. Recordings were made at values of the tilt angle θ ranging from 1.0° to 5.0° in steps of 0.25° . An example of the observed behaviour is given in figure 13, where a short section is shown of the time series which was recorded for $\theta = 4.0^\circ$.

The behaviour shown in figure 13 is made up of a large-amplitude oscillation on top of an apparently constant non-zero mean component. The latter feature is due

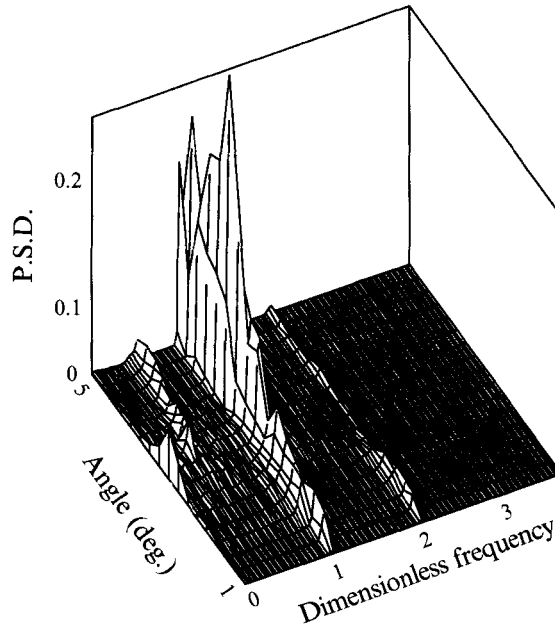


FIGURE 14. Power spectra obtained from experimental time series measured from fully developed nonlinear regime. Cylinder speed $\omega_1 = 10.67 \text{ rad s}^{-1}$, turntable speed $\omega_2 = 2.99 \text{ rad s}^{-1}$. Tilt angle varies from 1° to 5° in steps of 0.25° . Frequency axis scaled on forcing frequency $F = \omega_1/2\pi$.

to nonlinear boundary-layer effects, and will be discussed in detail elsewhere (Koblinc 1995). We choose to focus here on the oscillatory component of the response. In particular, it proves instructive to look at the power spectra which are obtained from the time series recorded at the various values of θ . Such information is displayed in figure 14.

The frequency axis of the power spectra is scaled on the forcing frequency $F = \omega_1/2\pi$. Several interesting features can be discerned when the fluid response is analysed in this manner. For all values of θ that were studied, the response exhibits a component at the forcing frequency. The response at the relatively small tilt angles between 1.0° and 2.5° is characterized simply by a peak at the forcing frequency F and one at the first harmonic at $2F$. Then, in an intermediate range between 2.5° and 3.5° , there is the presence of a very low-frequency component indicating dynamics in the flow which are taking place on a time scale that is much longer than that set by the forcing. The appearance of this low-frequency component is accompanied by a reduction in the amplitude of the harmonic at $2F$. Finally, for tilt angles between 3.5° and 5.0° , a subharmonic component emerges in the power spectra. This new component is at a frequency of approximately $F/2$. The amplitude is less than the fundamental component at F , but greater than the harmonic which has reappeared at $2F$.

The existence of these different response regimes is consistent with the observations made by Manasseh (1992) of qualitatively distinct routes by which inertial oscillations break down to irregular motion. In particular, the present measurements of dynamics with very long time scales for θ between 2.5° and 3.5° agrees with the flow-visualization characterizations of Manasseh. Furthermore, the present results provide further evidence to support the speculation first raised by McEwan (1971) that the 'resonant collapse' of inertial waves is a process which is caused by nonlinear interactions

between a small number of wave modes. Certainly, the emergence of a significant subharmonic response with increasing forcing amplitude is a feature which fits in with ideas relating to nonlinear finite-dimensional dynamical behaviour (see Thompson & Stewart 1986, for example).

7. Conclusions

The present study of flow in a rotating and precessing cylinder has provided a variety of quantitative results which are of use in assessing the validity of linear and inviscid approximations such as those adopted in a forthcoming paper by Tan & McIntyre (1995). Such assumptions, while facilitating numerical predictions of the fluid response to precessional forcing, are open to question given the inevitable presence of viscosity in real fluids and the observations of highly nonlinear breakdown phenomena which have been reported in previous experimental investigations.

The focus in this paper has been on those aspects of the fluid motion which relate to inertial wave phenomena. As far as this oscillatory behaviour is concerned, the present results support the use of linear inviscid theory in modelling the fluid response under conditions where the forcing is away from the primary resonance, and also for short times immediately following the onset of resonant precessional forcing. In this latter case, the growth of the oscillation amplitude was found to be linear for approximately the first ten tank rotations following the commencement of forcing. This linear growth rate is itself directly proportional to the tilt angle up to approximately 3° . Considering this fact together with the direct proportionality between oscillation amplitude and tilt angle for the case of quasi-impulsive forcing in §2, it is apparent that the present results are in accord with the observations made in drop tests of an exponential growth of nutation angle in the case of freely rotating tanks.

On the basis of the above experimental results, it would appear that the adoption of linear and inviscid approximations would be appropriate in a practical control system for establishing and maintaining the stability of rotating spacecraft with on-board liquid payloads. Given that the objective of such a control system is the correction of small departures of the nutation angle from zero, conditions would be such that any nonlinear effects in the inertial oscillations have insufficient time to develop. However, the validity of such an argument is open to question given the observations that, close to resonance, the fluid response is characterized not only by inertial oscillations but also by a mean azimuthal circulation. Such a flow must necessarily have implications for the net torque experienced by the tank. The behaviour and properties of this mean flow are the subjects of a future publication (Kobine 1995).

The author would like to thank Paul Linden, Richard Manasseh, Michael McIntyre and David Tan for useful discussions and suggestions throughout the course of this work. The expertise of the DAMTP technical staff is gratefully acknowledged, as is that of Professor S. Yoshida concerning laser Doppler velocimetry. Financial support was provided by the UK Science and Engineering Research Council.

REFERENCES

- BAINES, P. G. 1967 Forced oscillations of an enclosed rotating fluid. *J. Fluid Mech.* **30**, 533–546.
FULTZ, D. 1959 A note on overstability and the elastoid-inertia oscillations of Kelvin, Solberg and Bjerknes. *J. Meteorol.* **16**, 199–208.

- GLEDZER, E. B. & PONOMAREV, V. M. 1992 Instability of bounded flows with elliptical streamlines. *J. Fluid Mech.* **240**, 1–30.
- GREENSPAN, H. P. 1964 On the transient motion of a contained rotating fluid. *J. Fluid Mech.* **21**, 673–696.
- GREENSPAN, H. P. 1968 *The Theory of Rotating Fluids*. Cambridge University Press.
- HERBERT, T. 1986 Viscous fluid motion in a spinning and nutating cylinder. *J. Fluid Mech.* **167**, 181–198.
- JOHNSON, L. E. 1967 The precessing cylinder. In *Notes on the 1967 Summer Study Program in Geophysical Fluid Dynamics at the Woods Hole Oceanographic Inst.*, vol. 2, pp. 85–108.
- KELVIN, LORD 1880 Vibrations of a columnar vortex. *Phil. Mag.* **10**, 155–168.
- KOBLNE, J. J. 1995 Mean azimuthal circulation associated with inertial wave resonance in a rotating and precessing cylinder. In preparation.
- KUDLICK, M. D. 1966 On transient motions in a contained rotating fluid. PhD thesis, Massachusetts Institute of Technology.
- MALKUS, W. V. R. 1989 An experimental study of global instabilities due to the tidal (elliptical) distortion of a rotating elastic cylinder. *Geophys. Astrophys. Fluid Dyn.* **48**, 123–134.
- MANASSEH, R. 1992 Breakdown regimes of inertia waves in a precessing cylinder. *J. Fluid Mech.* **243**, 261–296.
- MANASSEH, R. 1993 Visualization of the flows in precessing tanks with internal baffles. *AIAA J.* **31**, 312–318.
- MCEWAN, A. D. 1970 Inertial oscillations in a rotating fluid cylinder. *J. Fluid Mech.* **40**, 603–640.
- MCEWAN, A. D. 1971 Degeneration of resonantly-excited standing internal gravity waves. *J. Fluid Mech.* **50**, 431–448.
- POCHA, J. J. 1987 An experimental investigation of spacecraft sloshing. *Space Commun. Broadcasting* **5**, 323–332.
- RUMYANTSEV, V. V. 1964 Stability of motion of solid bodies with liquid-filled cavities by Lyapunov's method. *Adv. Appl. Mech.* **8**, 183–232.
- STERGIOPOULOS, S. & ALDRIDGE, K. D. 1982 Inertial waves in a fluid partially filling a cylindrical cavity during spin-up from rest. *Geophys. Astrophys. Fluid Dyn.* **21**, 89–112.
- STERGIOPOULOS, S. & ALDRIDGE, K. D. 1987 Ringdown of inertial waves during spin-up from rest of a fluid contained in a rotating cylindrical cavity. *Phys. Fluids* **30**, 302–311.
- STEWARTSON, K. & ROBERTS, P. H. 1963 On the motion of a liquid in a spheroidal cavity of a precessing rigid body. *J. Fluid Mech.* **17**, 1–20.
- TAN, D. G. H. & MCINTYRE, M. E. 1995 Time-dependent integral-equation formulation for flow in spinning and nutating containers. In preparation.
- THOMPSON, J. M. T. & STEWART, H. B. 1986 *Nonlinear Dynamics and Chaos*. Wiley.
- VANYO, J., WILDE, P., CARDIN, P. & OLSON, P. 1995 Experiments on precessing flows in the Earth's liquid core. *Geophys. J. Intl* **121**, 136–142.